Molecular Therapy
Oncology
Original Article

Resistance signatures to oncolytic vesiculoviruses in pancreatic ductal adenocarcinoma

Chelsae R. Watters,[1,11] Oumar Barro,[1] Musa Gabere,[1,2] Mia Y. Masuda,[3] Natalie M. Elliott,[1] Elizabeth A. Raupach,[1] Khandoker Usran Ferdous,[4,5] Mulu Z. Tesfay,[4,5] Omeed Moaven,[6,7] Yumei Zhou,[1,2] Michael T. Barrett,[1,2,8,9] Kenneth H. Buetow,[10] Bolni Marius Nagalo,[4,5] and Mitesh J. Borad[1,2,8,9]

[1]Division of Hematology/Oncology, Department of Internal Medicine, Mayo Clinic, Scottsdale, AZ 85259, USA; [2]Department of Molecular Medicine, Mayo Clinic, Rochester, MN 55905, USA; [3]Department of Immunology, Mayo Clinic, Scottsdale, AZ 85259, USA; [4]Department of Pathology, University of Arkansas for Medical Sciences, Little Rock, AR 72205, USA; [5]The Winthrop P. Rockefeller Cancer Institute, UAMS, Little Rock, AR 72205, USA; [6]Division of Surgical Oncology, Department of Surgery, Louisiana State University (LSU) Health, New Orleans, LA 70112, USA; [7]Department of Interdisciplinary Oncology, Stanley S. Scott Cancer Center, LSU Health, New Orleans, LA 70112, USA; [8]Center for Individualized Medicine, Mayo Clinic, Rochester, MN 55905, USA; [9]Mayo Clinic Cancer Center, Mayo Clinic, Phoenix, AZ 85054, USA; [10]Computational Sciences and Informatics Program for Complex Adaptive System, Arizona State University, Tempe, AZ 85281, USA

Pancreatic ductal adenocarcinoma (PDAC) shows limited response to conventional therapies and immunotherapy due to dense stromal barriers and poor immunogenicity. Oncolytic vesiculoviruses hold therapeutic potential for PDAC by lysis of PDAC cells to release tumor-associated antigens, increasing tumor immunogenicity. We previously reported the efficacy of a chimeric vesicular stomatitis virus (VSV) expressing Morreton virus (MorV) glycoprotein in sarcoma. Here, we evaluated the oncolytic potency of MorV and chimeric virus, VMG, in PDAC models. VMG exhibited heterogeneous oncolysis across human PDAC cell lines and PDX cells, similar to parental viruses VSV and MorV. To evaluate potential signatures correlated with resistance to oncolytic vesiculoviruses, we compared transcriptomes of cell lines characterized as sensitive or resistant to oncolysis *in vitro*. We identified epithelial development and biological adhesion gene sets were significantly associated with vesiculovirus resistance. Additionally, escaped PDAC cells surviving two cycles of infection with VSV showed significant upregulation of stress keratins and downregulation of genes involved in retinoic acid metabolism and cell cycle. An overlapping 39 genes were higher in resistant cell lines at baseline as well as upregulated in escaped PDAC cells. Several resistance-associated genes are targets of anti-cancer therapies in development, offering potential combination approaches with oncolytic vesiculoviruses.

INTRODUCTION

The incidence of pancreatic ductal adenocarcinoma (PDAC), which comprises 85% of all pancreatic cancer cases, has increased over the past 40 years while the prognosis has remained poor.[1–3] Pancreatic cancer does not exhibit durable sensitivity to radiation, chemotherapy, and conventional immunotherapies.[4,5] These poor treatment responses can be attributed to a desmoplastic tumor microenvironment, consisting of a dense extracellular matrix (ECM) and cancer-associated fibroblasts (CAFs).[6] The dense stroma of PDAC leads to poor infiltration and suppression of dendritic cells and effector T cells, with a dominant presence of immunosuppressive regulatory T cells (Tregs), myeloid-derived suppressor cells (MDSCs), and tumor-associated macrophages (TAMs). The poor immunogenicity of PDAC and desmoplastic barrier to drug and effector T cell infiltration are significant challenges to therapeutic efforts.[7]

Oncolytic viruses (OVs) are a potential treatment option to improve immune activation within the PDAC tumor microenvironment through stimulation of innate and adaptive immunity, as well as increased presentation of tumor antigens.[8] OVs have been shown to increase therapeutic effect in combination with lower doses of gemcitabine, which can help reduce chemotherapy-related toxicity.[3] Several OV candidates are in clinical trials as monotherapies or combination therapies for pancreatic cancer. Preclinical evaluation of OV for PDAC has included herpesvirus, measles virus, reovirus, adenovirus, myxoma virus, Newcastle disease virus, vaccinia virus, and vesicular stomatitis virus (VSV).[3]

Vesiculoviruses such as VSV are an appealing OV platform due to their ease of genetic manipulation, independence from cell cycle, non-integration into the host genome, low seroprevalence, and oncoselectivity due to defective type I interferon (IFN) responses in some cancers.[9] The antiviral effects of type I IFNs have been well

Received 11 July 2024; accepted 14 January 2025;
https://doi.org/10.1016/j.omton.2025.200937.

[11]Present address: Boehringer Ingelheim Pharmaceuticals, Inc., Arlington, TX 76019, USA

Correspondence: Mitesh J. Borad, Division of Hematology/Oncology, Department of Internal Medicine, Mayo Clinic, Scottsdale, AZ 85259, USA.
E-mail: borad.mitesh@mayo.edu

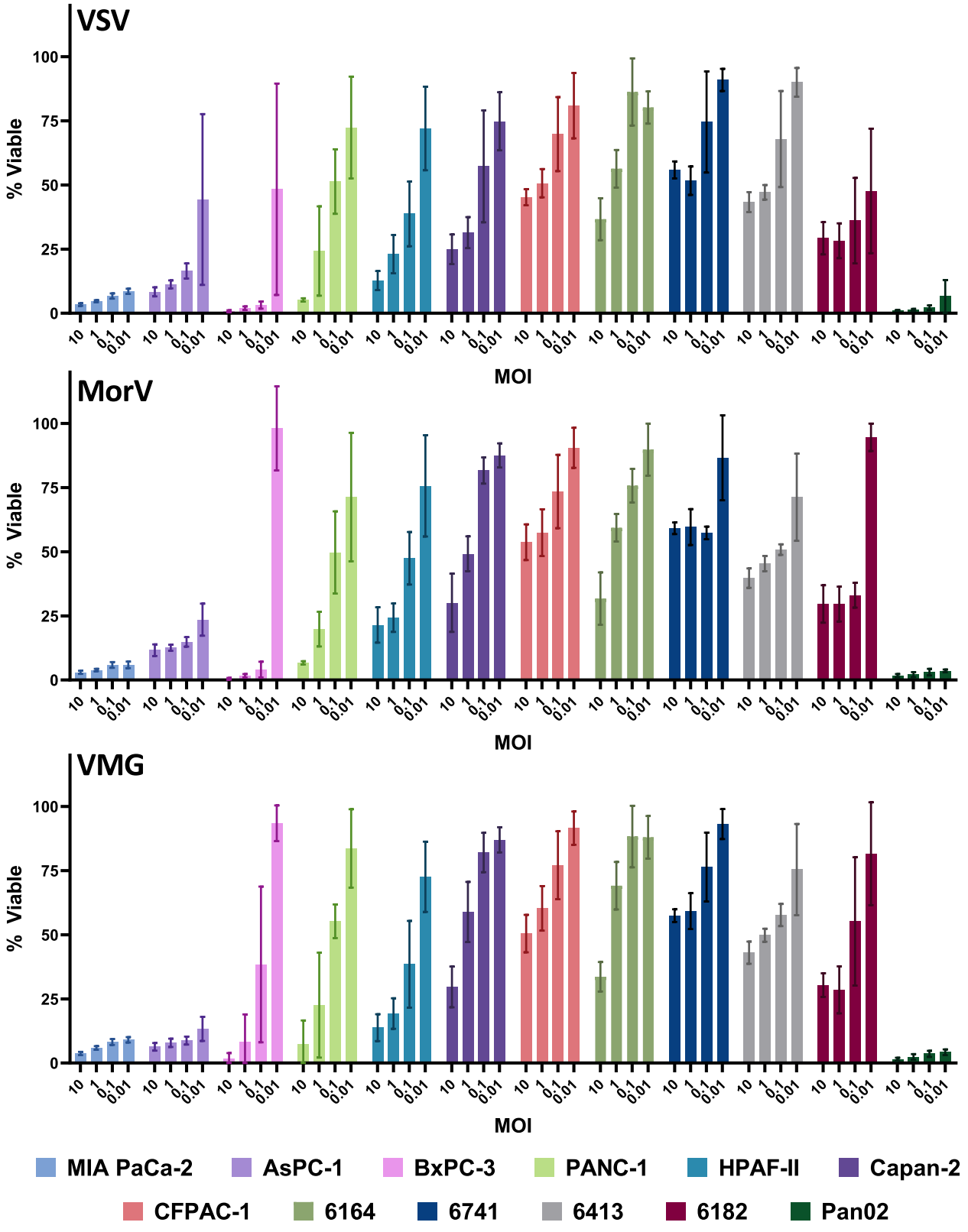

(legend on next page)

characterized in the context of cancer susceptibility to oncolytic vesiculovirus infection.[10–21] We and others have shown that several cancer models maintain responsiveness to type I IFN signaling, even if cells do not produce IFN in response to viral infection. We have observed variable cell viability outcomes *in vitro* when cancer cell lines are infected with members of the genus *Vesiculovirus*, including VSV. These variable levels of cell death are independent of cancer type or tissue of origin. We have shown previously that expression of the low-density lipoprotein receptor (LDLR) (which is the primary receptor for VSV), infectious viral progeny replication kinetics, or production of IFN-beta (IFNβ), do not fully explain differential cell killing across cancer cell lines.[22] The low production of type I IFN in these models can be due to specific pathway defects in cancer cells, or could be explained by viral-mediated blockade of transcription by the VSV matrix protein (M).[23] We hypothesized that cellular features beyond the type I IFN response and expression of interferon-stimulated genes (ISGs) contribute to variable susceptibility to oncolysis.

We have previously demonstrated oncolytic efficacy of a related vesiculovirus, Morreton virus (MorV), in models of hepatocellular carcinoma and cholangiocarcinoma (CCA).[24] Abrogated neurotoxicity compared with VSV following intranasal administration was shown by MorV, and also by a chimeric virus expressing the MorV glycoprotein in the VSV backbone, VMG.[22,24] Our group previously evaluated the chimeric virus VMG in multiple sarcoma subtypes, where it elicited oncolytic activity as well and notably increased intratumoral CD8+ T cell proportions in a syngeneic fibrosarcoma model.[22]

Here, we sought to evaluate the oncolytic potential of vesiculoviruses MorV and VMG in PDAC cell lines and PDX models. Furthermore, we evaluated treatment efficacy and immunophenotypic changes following intratumoral VMG administration in a syngeneic murine model of PDAC. We then utilized baseline expression data across cell lines to identify gene signatures associated with resistance. We further explored potential mechanisms of cancer escape by transcriptomic comparisons of derived PDAC cells surviving two cycles of infection with oncolytic VSV. The identification of these transcriptomic signatures is essential for guiding future viral engineering strategies and optimizing combination therapies. Furthermore, it can aid in identification of IFN-independent mechanisms of cancer cell escape from viral oncolysis, particularly in the context of viral infection-mediated selection pressure. These exploratory analyses can offer insights into mechanisms of resistance to improve development of oncolytic virotherapy for PDAC and other carcinomas.

RESULTS

MorV and VMG exhibit oncolysis across multiple PDAC cell lines

We evaluated the cytotoxicity of MorV and VMG across multiple human PDAC cell lines, PDX-derived cell lines, and a murine PDAC line at various multiplicities of infection (MOIs) using an MTS colorimetric readout of viability at 72 h post-infection (hpi). We compared the oncolytic effect of these novel viruses to VSV. We observed variable oncolysis across PDAC lines, which was highly correlated with starting dose of virus (Figure 1). We observed very similar remaining viability at 72 hpi with the three related vesiculoviruses. These data show that the oncolytic effect of VMG and MorV are similar to VSV. The highest level of resistance was exhibited by four PDX-derived lines (6164, 6741, 6413, and 6182), maintaining >25% viability 72 h after infection at MOI 10. Among PDAC cell lines, CFPAC-1 and Capan-2 exhibited the highest viability at 72 hpi, demonstrating greatest resistance to oncolysis. Human PDAC cell lines BxPC-3, PANC-1, and HPAF-II showed intermediate oncolysis, demonstrating resistance only at lower MOI. The human cell lines AsPC-1 and MIA PaCa-2 and murine cell line Pan02 were highly sensitive to oncolysis by all three viruses, even at the lowest MOI administered. Assessment of cytotoxicity by crystal violet assay showed remaining viable adherent CFPAC-1 and HPAF-II cells at 72 hpi (Figure S1). Overall, we observed that MorV and VMG had a similar oncolytic profile to VSV, and that some cell lines and all PDX models exhibited resistance to viral killing.

VMG productively infects and replicates in PDAC cell lines

To visualize successful viral entry and replication, we used a VMG construct encoding a reporter GFP gene (VMG-GFP). At 72 hpi with MOI 0.1, GFP fluorescence was detectable in all cell lines at variable levels (Figure S2). MIA PaCa-2 showed the greatest level of GFP expression at 72 hpi, as quantified by fluorescent area. These results show that VMG-GFP effectively entered and produced viral proteins, including virally encoded GFP, in PDAC cells. Despite the ability of the virus to productively infect in each cell line, some cell lines maintained >50% viability at 72 hpi (Figure 1).

We also observed that progeny of VMG reached infectious titers to similar levels as parental viruses VSV and MorV, as evidenced by plaque assays using supernatant from PDAC cells infected at MOI 0.1 (Figure S3). Viral titers reached 10e4–10e8 PFU/mL within 48 hpi in all PDAC cell lines assessed and levels were either similar or slightly decreased by 72 hpi. CFPAC-1 reached maximum viral titers between 10 and 24 hpi, potentially indicating a change in susceptibility to replication of virus within 24 h, as cells remained viable but without producing more virus, although virus was present. However, this indicates that there was not complete resistance at the start of infection since both virus and virally encoded GFP were produced by infected cells. Taken together, data from MTS assays and viral kinetics assays indicate similar profiles of the related vesiculoviruses in each cell line. Therefore, we propose that mechanisms driving resistance are similar for VSV, MorV, and VMG.

Figure 1. Oncolytic effects in PDAC with two related vesiculoviruses and chimeric VMG

Adherent cells were infected with VSV, MorV, or VMG at the indicated MOI. Viability was assessed by MTS colorimetric assay at 72 hpi by normalization to media-only controls. Bars represent the mean ± SD from nine replicates from three independent experiments per condition. Human cell lines: MIA PaCa-2, AsPC-1, BxPC-3, PANC-1, HPAF-II, Capan-2, CFPAC-1. PDX lines: 6164, 6741, 6413, 6182. Murine: Pan02.

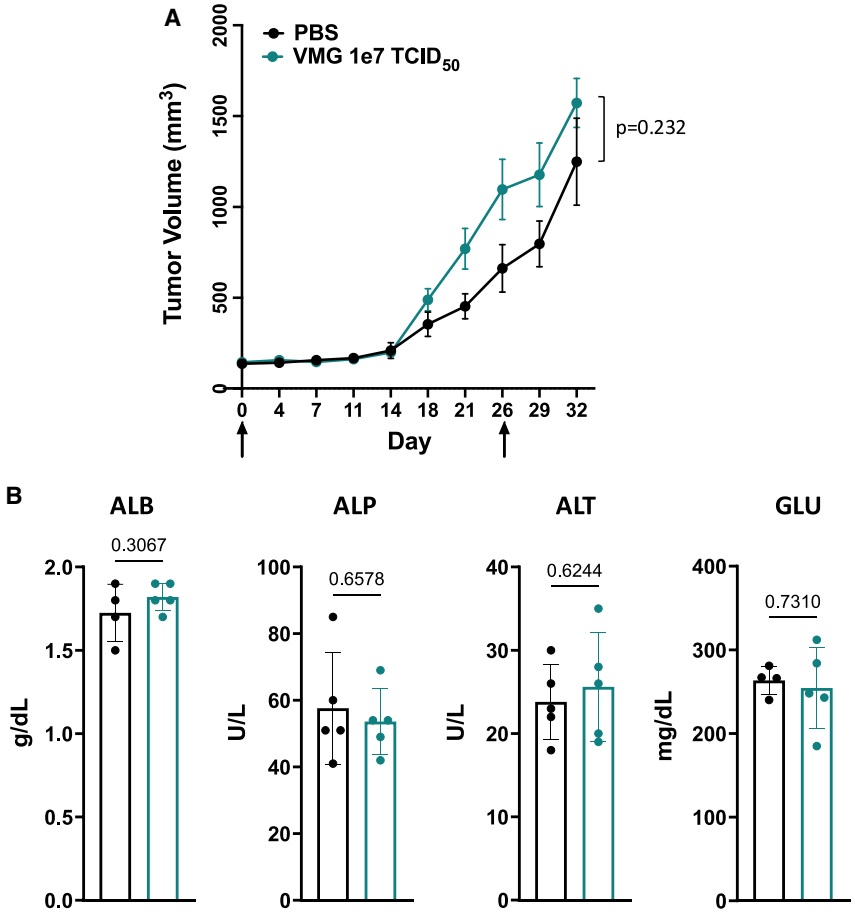

Figure 2. Evaluation of intratumoral injection of two doses of VMG in syngeneic flank tumor model of Pan02

(A) 3e6 Pan02 cells were subcutaneously implanted in the right hind flank of C57Bl/6 mice 7 days before the first injection of VMG. Mice were randomized and received an intratumoral injection of PBS or 1e7 $TCID_{50}$ VMG on day 0 and day 26. Points represent mean ± SD for $n = 7$ mice per group. p value was calculated by Welch's t test of the area under the curve. (B) Serum liver enzymes in blood collected at endpoint from treated vs. control mice. p values were calculated by unpaired t test. ALB: albumin, ALP: alkaline phosphatase, ALT: alanine aminotransferase, GLU: glucose.

Pan02 tumor immune landscape changes following VMG administration

We next evaluated oncolytic potential of VMG treatment of PDAC *in vivo*. Pan02 was shown to be the most susceptible cell line to oncolysis *in vitro*, showing minimal cell viability at 72 hpi with VMG. Since Pan02 was the only murine cell line in the initial screen, we also evaluated the susceptibility of another murine PDAC model, KPCY. We found KPCY exhibited higher viability post-infection with VMG-GFP (~50% viability with MOI 10), so did not pursue this model for *in vivo* evaluation (Figure S4). Murine Pan02 cells were subcutaneously implanted in the right hind flank of immunocompetent C57BL/6 mice. Mice were randomized to receive either intratumoral injection of VMG (treatment group) or phosphate-buffered saline (PBS) (control group). A single intratumoral dose of VMG did not significantly affect the rate of tumor growth *in vivo*, and a delayed second dose at day 26 did not affect tumor volume before end-of-study at day 32 (Figure 2A). The safety of intratumoral VMG dosing in this immunocompetent model was also evaluated. Viral administration was well tolerated with no adverse events in the VMG-treated mice as evidenced by body weight (Figure S5) and serum liver enzyme levels (Figure 2B). No significant differences were observed for either of these parameters. One mouse in the control group reached humane endpoint before end-of-study due to tumor ulceration on day 21. While VMG was highly cytotoxic in the Pan02 *in vitro* model, no significant tumor regression *in vivo* was achieved.

The discrepancy between the oncolytic effect of VMG infection on the Pan02 cell line and the syngeneic tumor model indicates extrinsic factors contributing to therapeutic resistance *in vivo*. To investigate possible reasons for lack of tumor inhibition in the syngeneic model Pan02, we tested the responsiveness of the cell line Pan02 to exogenous IFNβ that may have been produced by surrounding and infiltrating murine cells within the tumor following injection of the virus. We observed that Pan02 cells were protected from oncolysis in the presence of mIFNβ at levels higher than 500 U/mL (Figure S6). This indicates the potential of protection arising from other IFN-competent cells within the tumor microenvironment and is consistent with previous reports.[25] Tumors that maintain response to IFN, even if IFN production is defective, may not be ideal candidates for oncolytic vesiculovirus therapy.

VMG-treated Pan02 tumors exhibited an altered landscape of tumor infiltrating leukocytes (TILs) at experimental endpoint as visualized by t-distributed stochastic neighbor embedding (t-SNE) (Figure 3A). These changes consisted of a decrease in CD11b and F4/80 expressing cells that made up most of the infiltrating CD45 population, as well as an increase in the CD8 and IA/IE expressing compartments (Figure 3B). Changes in TIL frequencies were confirmed and quantified by manual subset gating (Figures 3C and S7). A significant decrease in the proportion of CD11b+ cells within the CD45 compartment ($p = 0.0279$) was observed. Among these CD11b+ cells, the proportion of F4/80+ CD206+ tumor-associated macrophages (TAMs) also decreased but was not significant ($p = 0.0725$). Of the CD11b+ cells that remained in the tumor, there was a noticeable increase in the Class II MHC (IA/IE) expression. The mean proportion of CD3+ T cells

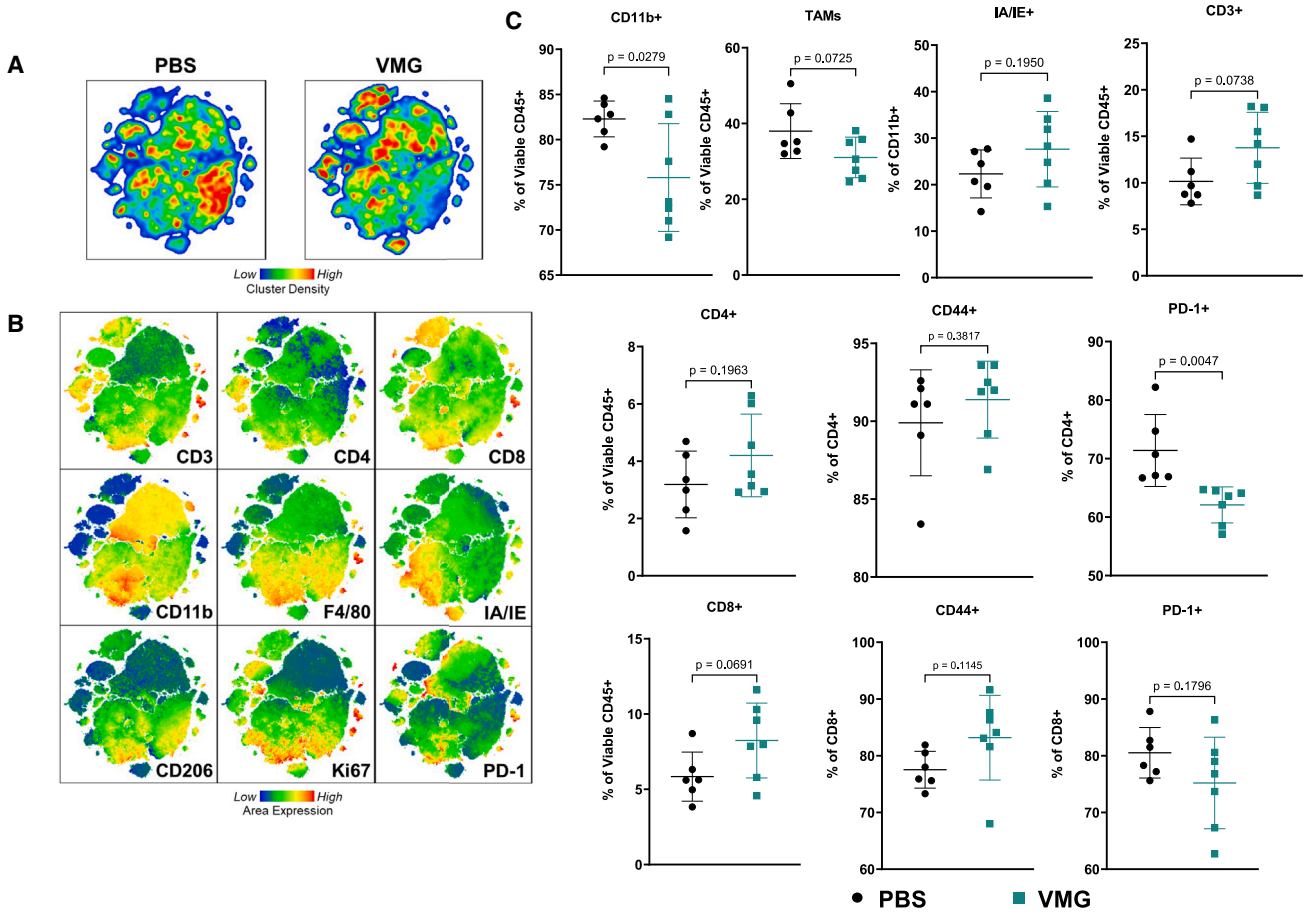

Figure 3. Immune landscape changes in TILs within Pan02 after intratumoral VMG administration

(A) t-SNE clustering analysis of 4e4 TILs (Viable CD45+) per tumor in PBS ($n = 6$) and VMG-treated ($n = 7$) mice from Figure 2. Heatmap indicates density by number of cells in each region. (B) Heatmap expression for level of expression of cell markers in each region. (C) Comparison of immune subsets by manual gating. Significance was calculated by unpaired t test. TAMs: tumor-associated macrophages (CD11b+/F4/80+ CD206+). Representative gating strategy for subsets is shown in Figure S7.

was increased in VMG-treated tumors. Additionally, PD-1 was significantly decreased on CD4+ T cells ($p = 0.0047$). A trend toward reduced expression of PD-1 was also observed for CD8+ T cells, although this did not reach statistical significance ($p = 0.1796$). We observed no statistical difference in the proportions of antigen-experienced (CD44+) CD4s or CD8s. Despite the modest immunogenic changes that VMG elicited, it was not sufficient to lead to tumor regression. These results indicate that the majority of immune cells infiltrating Pan02 tumors were myeloid subsets that may be immunosuppressive.

Biological adhesion and epithelium development gene signatures are associated with vesiculovirus resistance

The type I IFN pathway has been well-documented in its contribution to resistance to oncolytic vesiculoviruses. We sought to unbiasedly identify additional factors that may contribute to variable levels of cell death following replicative VSV (or VMG) infection. To do this, we identified shared baseline transcriptomic features of cancer cell lines that were correlated with a VSV-resistant or -sensitive phenotype. We classified 26 cell lines across cancer types ($n = 12$ resistant and $n = 14$ sensitive) using a cutoff of a mean viability greater than 50% at 72 hpi with laboratory strain VSV Indiana at MOI 0.1 (Table 1). No associations were seen between sensitivity and whether the cell lines were derived from primary tumor or metastases, sex of the original patient, or cancer driver mutation (data not shown). We then utilized publicly available baseline transcriptome data from DepMap (https://depmap.org/portal/) to compare gene expression in cell lines characterized by our group as sensitive or resistant.

Many pancreatic cancer cell lines evaluated for their response to oncolytic VSV were classified as resistant. Differential expression analysis was performed using significance analysis of microarrays and RNA sequencing (SAM-R). We identified 203 genes as significantly more highly expressed in resistant lines and 38 genes that were more lowly expressed in resistant lines as compared with

Table 1. Cell lines used in DepMap comparison of sensitive and resistant cell lines

DepMap ID	Cell line	Mean % viability 72 hpi	Classification	Origin
ACH-000354	Capan-1	0	Sensitive	Pancreas
ACH-000483	SNU-182	0	Sensitive	Liver
ACH-000739	HepG2	0	Sensitive	Liver
ACH-000808	Huh-28	0	Sensitive	Bile duct
ACH-000052	A673	5	Sensitive	Bone
ACH-000480	Huh7	5	Sensitive	Liver
ACH-000958	SW48	5	Sensitive	Colorectal
ACH-001536	KKU-100	5	Sensitive	Bile duct
ACH-001858	SSP-25	5	Sensitive	Bile duct
ACH-000681	A549	10	Sensitive	Lung
ACH-000552	HT-29	12	Sensitive	Colorectal
ACH-000182	SNU-869	20	Sensitive	Bile duct
ACH-000601	MIA PaCa-2	25	Sensitive	Pancreas
ACH-000939	SK-UT-1	30	Sensitive	Soft tissue
ACH-000164	PANC-1	50	Resistant	Pancreas
ACH-000625	Hep3B	50	Resistant	Liver
ACH-000138	CFPAC-1	55	Resistant	Pancreas
ACH-000145	SK-LMS-1	55	Resistant	Soft tissue
ACH-000976	HuCCT-1	55	Resistant	Bile duct
ACH-001673	TFK-1	55	Resistant	Bile duct
ACH-000141	SNU-308	65	Resistant	Bile duct
ACH-000377	SNU-478	70	Resistant	Bile duct
ACH-001853	KMCH-1	70	Resistant	Bile duct
ACH-000094	HPAF-II	75	Resistant	Pancreas
ACH-000178	Hs766T	80	Resistant	Pancreas
ACH-000535	BxPC-3	90	Resistant	Pancreas

Cell line mean viability 72 hpi in MTS assay with VSV Indiana at MOI 0.1 and classification.

sensitive lines (raw-p < 0.05, fold change >1) (Figure 4). The gene with the lowest raw-p value for significantly higher expression in resistant lines was *HAS3* (hyaluronan synthase 3), and the greatest fold change expression was *WNT7A* (Wnt family member 7A), followed by *DHRS9* (dehydrogenase/reductase 9). The top three genes more highly expressed in resistant cell lines (*WNT7A*, *DHRS9,* and *HAS3*) are unfavorable prognostic indicators in pancreatic cancer (Figures S8A–S8C).[26] In contrast, a gene with significantly lower expression in resistant lines, *LIMS2* (LIM zinc finger domain containing 2) is associated with better outcomes in pancreatic cancer and prognostic for favorable outcomes in liver cancer. These results may indicate a possible relationship between cancer cellular resistance to oncolytics and poor patient outcomes (Figure S8D). *HAS3* was an interesting finding, as its product hyaluronic acid is known to have antiviral properties.[27] A direct correlation between *DHRS9* or *WNT7A* with viral resistance is not currently known.

We additionally performed gene ontology (GO) analysis to identify biological processes enriched within the DEGs. The GO Biological Processes significantly enriched in 203 genes more highly expressed in resistant lines were biological adhesion and epithelium development (Table S3). The 38 genes that had lower expression in resistant lines did not yield significant biological process enrichment. A relationship between biological adhesion and course of viral infection has not been described. However, a relationship between cell adhesion and cancer therapy resistance has been previously demonstrated.[28] We therefore propose there may be shared cancer mechanisms of resistance to oncolytic vesiculoviruses and other conventional cancer therapies.

Viral proteins are primarily upregulated in early infection in PDAC lines

We also evaluated the distinctions between sensitive and resistant PDAC lines by comparing protein upregulation in a cell line of each classification at 18 hpi. At this time point, the most differentially expressed proteins were viral, even in CFPAC-1, which is resistant to subsequent cell death (Figure S9). These results indicate that all viral structural proteins are produced in resistant lines, although the fold changes of all viral proteins were lower in CFPAC-1 (resistant) vs. MIA PaCa2. The only non-viral protein significantly upregulated in CFPAC-1 was paralemmin-1 (PALM), while Gem nuclear organelle associated protein 7 (GEMIN7) was downregulated. In sensitive line MIA PaCa2, A-kinase anchoring protein 9 (AKAP9) was upregulated. The relationship of these proteins to the course of viral infection is indeterminate. Notably, proteins related to the type I IFN antiviral response were not detected as significantly upregulated by this analysis.

Epithelium stress response, O-Glycan processing and retinoid metabolism pathways altered in vesiculovirus-escaping PDAC cells

To determine transcriptomic changes or enrichment associated with cancer cell survival after oncolytic virus infection, we performed RNA sequencing (RNA-seq) comparing parental vs. virus-exposed PDAC cell lines (CFPAC-1, BxPC-3, and Capan-2). We elicited two rounds of selective pressure with VSV infection at MOI 0.1 in resistant PDAC cells. We then performed bulk RNA-seq on the surviving cells to compare their transcriptomic profiles with the parental uninfected cell line.

In post-infected CFPAC-1 cells, numerous ISGs were upregulated, including *STAT2, OAS1, MX1, IRF7,* and *RSAD2* (Figures 5 and 6). Although *IFNβ* mRNA expression was significantly increased in the derived cells, *IFNλ3* expression appeared to be even more highly upregulated (Figures 5 and 6). In addition, *IFNλ1* and *IFNλ2* were also significantly upregulated (Figures 5 and 6).

Additionally, several genes that are not known to be related to canonical antiviral interferon pathways were differentially expressed (Figures 5, 6, S10, and S11).[29] The most significantly upregulated genes in post-infected cells were *KRT16* and *KRT17*, genes associated

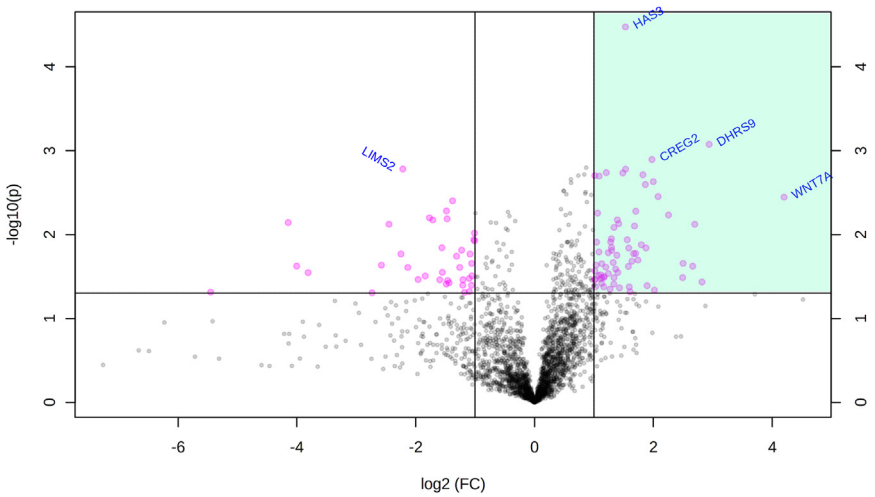

Figure 4. DEGs in cell lines resistant to oncolytic VSV over sensitive cell lines from publicly available RNA-seq data

Genes were filtered for the top 25% variance and analyzed using significance analysis of microarrays and RNA-seq (SAM-R). Area in green shows 203 genes that are significantly more highly expressed in resistant lines (fold change >1, raw-p < 0.05).

with the squamous epithelium stress response (Figures 5 and 6). *KRT16* is prognostic in pancreatic cancer, where high mRNA expression is associated with lower patient survival (Log rank p value = 0.000011) (Figure S12).[26] Additionally, expression of *PVRL4*, the gene encoding the epithelial cell measles virus receptor, was increased. As measles virus (MeV) is also in development as an oncolytic platform, this may allow for improved targeting of MeV, or MeV-pseudotyped viruses, to vesiculovirus-resistant PDAC tumors.[30]

The top three downregulated genes in derived resistant CFPAC-1 cells were *DHRS3*, *RBP1*, and *STRA6*, all of which are involved in retinoid metabolism (Figures 5, 6, and S11). Although not identified as associated by STRING analysis, the next most significant downregulated gene *SERPINA5* has been shown to bind retinoic acid.[31] Other downregulated genes included *RRM2* (ribonucleotide reductase small subunit M2), which contributes to DNA replication and repair, and *SNAI2* (Slug), which is involved in EMT.[32,33]

We also derived resistant cells for BxPC-3 and Capan-2 to determine if similar changes arose in these cell lines after two cycles of infection with VSV. Capan-2, like CFPAC-1, showed upregulation of *IFNL1*, *-2*, and *-3*, as well as *IFNβ1* (Figures 6A and 6B). In contrast, BxPC-3 did not show upregulation of mRNA expression of the type I or type III IFNs. Capan-2 also showed increased expression of several keratins, including *KRT6A*, *KRT16*, and *KRT17* (Figure 6). *KRT16* expression was also increased in BxPC-3 cells upon infection. BxPC-3 exhibited the highest expression of *KRT6A* and *KRT17* at baseline. *SPRR3* and *TRIM29* were increased with each cycle of infection in all three cell lines. The downregulation of retinoid metabolism-related genes *DHRS3*, *RBP1*, and *STRA6* was observed in all the three cell lines. The greatest fold changes in gene expression were seen in CFPAC-1 and Capan-2 after two cycles of infection (Figure 6B).

We then compared the 539 genes that were significantly upregulated in derived resistant CFPAC-1 lines with the 203 genes identified to be associated with resistant cell lines at baseline. From these two sets of genes, we identified 39 genes to be shared (Figure 7A). These included *MUC1*, *MUC16*, *MSLN*, *SFN*, *ITGB4*, *IRF6*, *TACSTD2*, *KRT15*, *DSG3*, *TRIM29*, *WNT7A*, and *WNT10A* (Figure 7B). The identified functional enrichments by these genes recapitulated the epithelium development biological process we had previously identified, as well as O-glycan processing.

DISCUSSION

In this study, we evaluated the oncolytic potential of a chimeric virus, VMG, across multiple PDAC models. We observed oncolysis across human PDAC cell lines and PDX lines, although some exhibited resistance to viral-induced cell death depicting the heterogeneity of vesiculovirus oncolysis in pancreatic cancer as has been previously described.[9,10,15] Notably, we observed very similar profiles of sensitivity and resistance to laboratory strain VSV Indiana, wild-type MorV, and chimeric VMG. This indicates that the switching of VSV-G to the MorV glycoprotein does not attenuate the oncolytic capabilities of the vector. Despite observance of resistance to cell death, all three vesiculoviruses were able to infect and produce infectious viral progeny in both sensitive and resistant cell lines as evidenced by plaque assay. Viral protein expression was visualized by GFP fluorescence after infection with VMG-GFP to variable levels in PDAC cell lines. This highlights that the resistance to virally induced cell death is not due to inability of the virus to either enter the cells or to productively replicate and other factors must contribute to differences in infection outcome.

In vitro evaluation showed the murine Pan02 cell line was exceptionally sensitive to viral oncolysis. However, this sensitivity did not translate to tumor regression in a syngeneic murine model of Pan02 following VMG administration. This suggests that the tumor microenvironment may be impeding the oncolytic effectiveness of VMG. Several challenges to oncolytic virotherapy, which likely contributed to the lack of tumor regression *in vivo*, are well-recognized. These include inefficient viral distribution within the tumor, reduced infection efficacy due to tumor hypoxia, an immunosuppressive tumor microenvironment, and the presence of strong intracellular antiviral defense mechanisms.[35]

As we have previously postulated, an intact responsiveness to exogenous IFNβ may instill resistance to oncolytic VMG *in vivo*.[22] This

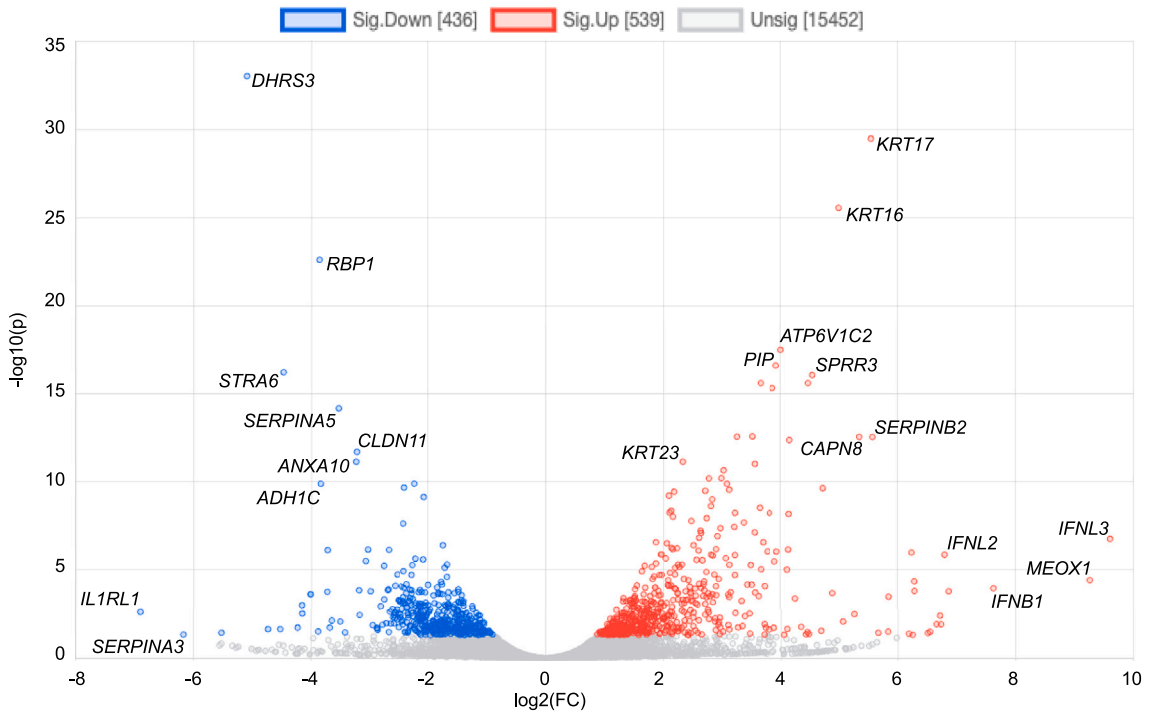

Figure 5. DEGs in derived resistant CFPAC-1 vs. parental CFPAC-1

Volcano plot of differentially expressed genes comparing uninfected to post-infected CFPAC-1 cells using DESeq2 analysis of RNA sequencing data, using experimental duplicates. Genes showing fold change>1 with an adjusted $p < 0.05$ were considered significant.

hypothesis is supported by prior work showing that CAFs and TAMs can respond to viral infection via secretion of IFNβ in ovarian and breast tumors, mediating resistance to oncolytic virotherapy.[25] This mechanism can be overcome by administration of JAK/STAT inhibitors such as ruxolitinib to prevent downstream signaling in response to IFNs.[10,36] Further work is necessary to abrogate the effect of stromal cell antiviral responses in oncolytic resistance. Other factors may contribute to therapeutic resistance *in vivo*, such as mechanical barrier of extracellular matrix preventing viral spread. The mechanical barrier of PDAC, particularly hyaluronic acid, has previously been successfully targeted by administration of pegylated hyaluronidase (PEGPH20).[37–39] Degradation of hyaluronans by this enzyme would have an added benefit in the context of virotherapy, as hyaluronic acid has known antiviral properties.[27] However, PDAC stroma is complex, composed of collagens, integrins, proteoglycans, glycoproteins, and proteases. Therefore, simultaneous targeting of these components could enhance treatment efficacy in PDAC.

VMG administration did not elicit any observable signs of toxicity in an immunocompetent model, consistent with previous results we reported in a murine model of sarcoma. As others have reported, not all cancers are defective in their type I IFN response.[40] We did observe significant changes in tumor immune infiltration after VMG therapy, including a significant decrease in CD11b+ cells and an increase in T cells and antigen-presenting cells, as well as a decrease in PD-1 expression on T cells, particularly on CD4s. We hypothesize that T cells in untreated tumors would exhibit elevated PD-1 expression from chronic tumor antigen stimulation. In contrast, after oncolytic administration, newly infiltrated T cells will upregulate PD-1 only immediately after activation and then PD-1 levels will decrease as virus is cleared.[41] TILs in our study were collected 6 days after final oncolytic administration, and therefore PD-1 levels in newly infiltrated T cells that have not been chronically stimulated would return to baseline expression of PD-1. One limitation to our immunophenotyping data is that it may be biased by changes in the distribution of immune cells, not by quantification of absolute counts per milligram of tumor. These data show the potential for effective combination therapy for VMG by altering the immunosuppressive microenvironment. In the future, VMG will be evaluated in further PDAC models with defective IFN responses with efforts to optimize therapeutic efficacy.

An additional goal of this study was to identify inherent features or gene expression changes in PDAC cells resistant to oncolytic vesiculoviruses. Gene expression patterns associated with resistance to therapy that are identified can be leveraged to hypothesize rational combination therapy. Here, we utilized several hypothesis-generating methods to identify possible features of vesiculovirus resistance in PDAC cells, which may be shared across cancers of epithelial lineage. Overall, we detected an epithelial development gene set by RNA-seq comparison of both publicly available data from sensitive and resistant cell lines, and of derived VSV-resistant PDAC cells.

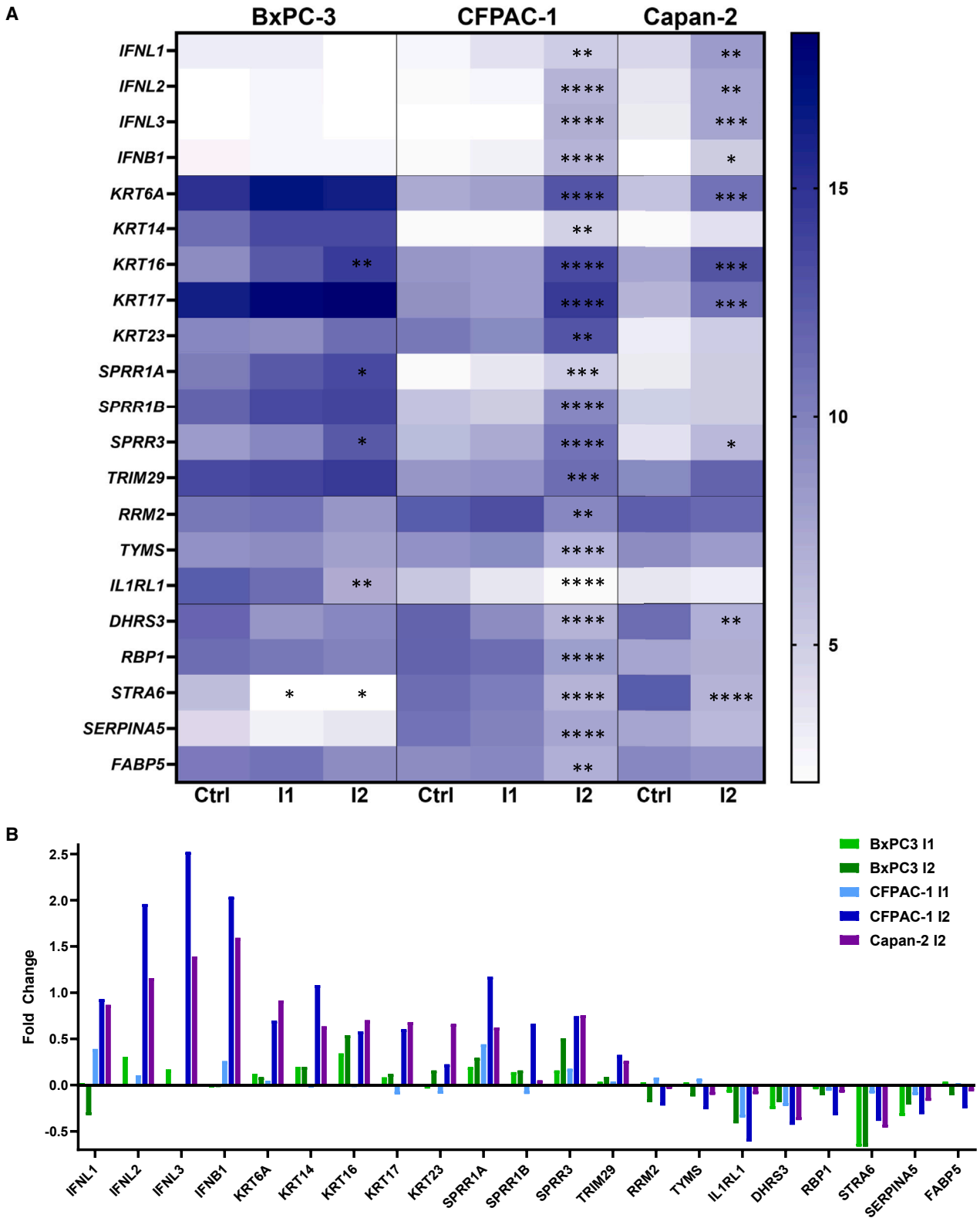

(legend on next page)

We found that type III IFNs (IFNλ1, IFNλ2, and IFNλ3) were significantly upregulated in resistant CFPAC-1 cells as compared with other PDAC cell lines, suggesting a synergistic antiviral role with type I IFNs. Although both type I and III IFNs induce antiviral states, increased concentrations of type III IFNs are often required for similar antiviral effects *in vitro*.[42] IFNλ primarily affects epithelial and certain immune cells like neutrophils, playing a crucial role in defending against viral invasion at mucosal surfaces.[43] While the type I IFN response is rapid yet transient, the type III response is slower but more sustained and less inflammatory, focusing on epithelial and barrier surfaces.[44] Type III IFNs also show anti-proliferative and antitumor activities *in vivo* and reduce VSV infectivity.[45] However, they can also mediate antitumor immune responses post-VSV oncolytic therapy in immunocompetent murine models.[46] Therefore, overcoming type III IFN production might be essential to counter PDAC resistance to oncolytic vesiculoviruses.

KRT16 and *KRT17* were also highly upregulated after two cycles of VSV infection in CFPAC-1. Importantly, the expression of keratins and IFN-lambda (IFN-λ) are exclusive to epithelium. KRT6, KRT16, and KRT17 are typically absent in healthy epidermis but are upregulated in inflammatory conditions.[47] Various cytokines, including tumor necrosis factor-α, epidermal growth factor, transforming growth factor-α, interleukin-1, and IFN-γ, induce the expression of these stress keratins, highlighting their role in cutaneous inflammatory responses. However, their function in the context of oncolytic infection remains unclear.

MUC1 (mucin 1) was shown to be central to a network of 39 genes that were upregulated in derived resistant CFPAC-1 cells and upregulated in a panel of oncolytic-resistant cancer cell lines. MUC1 expression can mediate resistance of cancer cells to chemotherapy, and has also been shown to inhibit influenza, poxvirus, rotavirus, HIV, and adenovirus.[48–51] VSV-ΔM51 infectivity is reduced in PDAC cells overexpressing MUC1.[48] Our results support this previous finding that MUC1 has a role in PDAC resistance to oncolytic vesiculoviruses. *MSLN* (mesothelin) was also identified in the 39 shared genes between derived resistant and baseline resistant cell lines. Both MUC1 and mesothelin have previously been identified as biomarkers for predicting survival in pancreatic cancer by immunohistochemistry (IHC).[52] Another mucin, *MUC16*, was also shown to be higher in resistant lines as well as upregulated in derived resistant cells. A previous study evaluated surface expression of MUC16 on three PDAC cell lines Capan-1, Capan-2, and MIA PaCa-2, where Capan-2 was shown to have the highest expression of MUC16, whereas MIA PaCa-2 lacked surface expression of MUC16.[53] This corroborates our data by demonstrating that a resistant cell line expresses higher levels of MUC16. MUC16 has also been shown to have a role in ovarian cancer resistance to genotoxic drugs (cisplatin, cyclophosphamide, doxorubicin, and etoposide) but not microtubule-targeting drugs (paclitaxel and vinorelbine).[54] ITGB4, also identified in the 39 shared genes, is important to identifying partially mesenchymal carcinoma cells.[55] It is also associated with poor prognosis in pancreatic cancer.[26,56]

The top significant gene more highly expressed at baseline in resistant cell lines was *HAS3* (hyaluronan synthase 3), although this gene was not included in any of the epithelium development or adhesion gene sets. Interestingly, hyaluronic acid is a major component of the extracellular matrix and has antiviral properties. It is also prognostic in pancreatic cancer, associated with poor outcomes.[26,56] *HAS3* was previously shown to be the most significantly downregulated gene in resistant pancreatic cell line Hs766T following treatment by IKK-2 inhibitor TPCA-1, which increased PDAC sensitivity to oncolytic VSV-ΔM51.[57] However, we saw *HAS3* expression decreased in derived resistant CFPAC-1 cells.

We also observed that *RRM2* (ribonucleoside-diphosphate reductase subunit M2) was downregulated in derived resistant CFPAC-1 cells. RRM2 has recently been identified as a tumor promotor and therapeutic target.[32] RRM2 is thought to mediate resistance to many chemotherapeutic drugs and inhibition of RRM2 in tumors may mediate chemosensitization.[58] Previous studies have reported that the organic molecule osalmid could act as an RRM2 inhibitor and had synergistic antitumor effects with radiation in *in vitro* and *in vivo* models of esophageal cancer. The downregulation of RRM2 we observed after VSV treatment in resistant cells may indicate that these cells would be more sensitive to chemotherapy or radiation. Given that RRM2 downregulation can confer sensitivity to nucleoside analogs such as gemcitabine, a standard of care in pancreatic cancer, there is impetus to explore rational combinations of vesiculoviruses with gemcitabine-based treatment. Further work would entail evaluating whether the downregulation of RRM2 is observed in the setting of clinical trials.

Another target arising in resistant cells is *TACSTD2*, encoding trophoblast cell surface antigen 2 (Trop2). Trop2 is a transmembrane glycoprotein and calcium signal transducer that is overexpressed in some tumors while expression is limited in normal tissues.[59] Furthermore, it is primarily expressed in epithelial cells. It has been shown to be involved in signaling pathways leading to tumor development, invasion, and metastasis. An anti-Trop2 antibody-drug conjugate (Trodelvy, sacituzumab govitecan) has been developed and approved to treat metastatic triple-negative breast cancer and bladder cancer. Our results indicate that this antibody-drug conjugate against Trop2 could potentially target PDAC cells that are resistant to

Figure 6. Shared differentially expressed genes across post-VSV-infected resistant PDAC cell lines

(A) Heatmap of expression of selected genes of interest across PDAC cell lines after VSV infection. Data are normalized to counts per million (CPM). Ctrl is uninfected cell line expression of each gene. I1 is performed on surviving cells 72 hpi with VSV (MOI 0.1). I2 is derived resistant cells 72 hpi with the second course of VSV infection (MOI 0.1). Statistics are calculated by two-way ANOVA comparing with the Ctrl condition. $^{*}p < 0.05$, $^{**}p < 0.005$, $^{***}p < 0.001$, $^{****}p < 0.0001$. (B) Fold change over control for each gene in infected conditions.

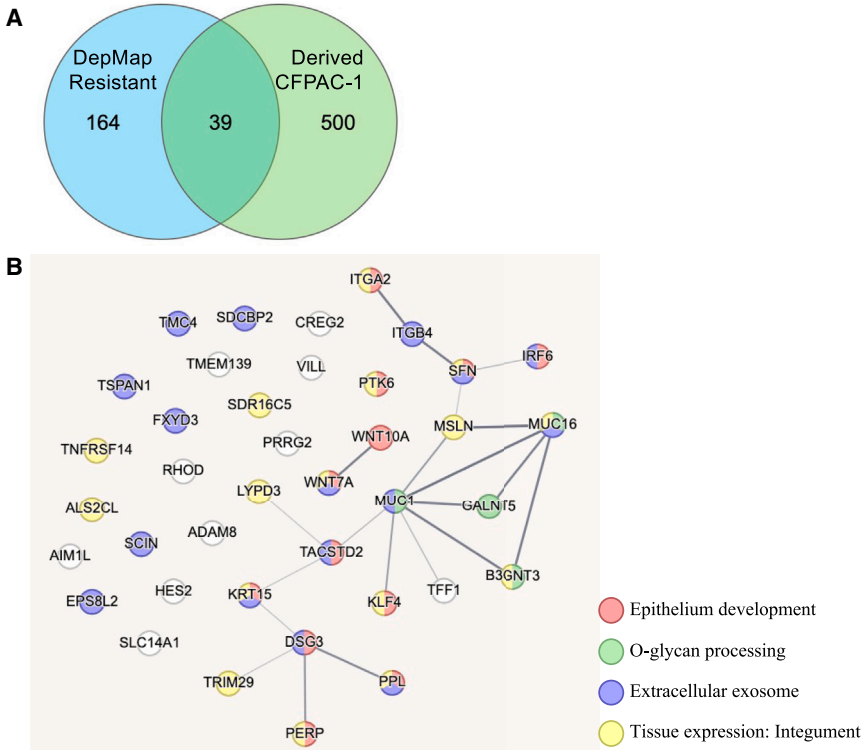

Figure 7. Overlapping genes between cell lines resistant to VSV-induced oncolysis at baseline and genes upregulated in derived resistant CFPAC-1

(A) Venn diagram showing that 39 genes are shared as significantly higher in resistant cancer cell lines at baseline and upregulated in a resistant cell line after two rounds of infection with VSV. (B) STRING Network analysis of 39 genes. Functional enrichments are as follows: Biological Process: Epithelium development (red) and O-glycan processing (green). Cellular Component: Extracellular exosome (purple). Tissue expression: Integument (yellow). Analyzed in string-db.org.[34]

oncolytic vesiculoviruses and be considered for a combination therapy approach through further preclinical and pilot clinical studies.

These signatures will need to be further validated in other PDAC models, as well as whether they are present across resistant cancer types. Notably, the signatures observed here may be exclusive to resistance to RNA viruses, as a previous similar study deriving cancer cells resistant to herpes simplex virus-based oncolytic, G207, yielded differently regulated gene signatures in resistant cells.[60]

In the initial screening across multiple cancer types, there were relatively few DEGs identified with modest *p* values and fold changes, most likely due to the heterogeneity at baseline across cell lines. Further research will be required to verify the epithelial gene signatures identified in resistant cells by protein expression assays such as flow cytometry or immunoblotting, and to determine which of these serve a functional role in allowing cancer cells to resist vesiculovirus infection. Genetic knockout or knockdown experiments of the identified genes could further elucidate their involvement in vesiculovirus resistance. Additional approaches such as single-cell RNA-seq are needed to determine whether overexpression of genes driving these epithelial signatures is present at baseline in a subpopulation of cells or if their expression is induced upon infection. We hypothesize that heterogeneity exists at baseline within each cell line that contributes to viral response or escape variants to OVs. This hypothesis is supported by a previous study showing that cellular heterogeneity exists in pan-cancer cell lines that recapitulates transcriptional programs observed in human tumors.[61] A limitation to this study is that we induced the selective pressure for derivation of resistant cells *in vitro*, so our results may not fully recapitulate the breadth of selective pressures that PDAC cells experience within the tumor microenvironment.

Overall, we have shown that resistance to oncolytic vesiculoviruses is multi-factorial. Our work identifies putative markers and signatures for vesiculovirus resistance and an array of combinatorial approaches for further evaluation in vesiculovirus-resistant PDAC. Notably, several of these genes are also prognostic markers in pancreatic cancer. The transcriptomes of vesiculovirus escape PDAC cells yield several therapeutic targets for which drugs are already in development. Our findings warrant further exploration of the mechanistic role in resistance of these signatures as well as combination therapies targeted to the identified genes associated with resistance. These investigations will enable rational testing of combination therapies and improve viral engineering strategies to circumvent or target the elucidated mechanisms.

MATERIALS AND METHODS

Cell lines

BxPC-3, CFPAC-1, HPAF-II, MIA PaCa-2, and PANC-1 were purchased from ATCC (Manassas, VA). AsPC-1 and Capan-2 were generously provided by Dr. Martin Fernandez-Zapico (Mayo Clinic, Rochester, MN). Pan02 was obtained from the Division of Cancer Treatment and Diagnosis Tumor Repository of the National Cancer Institute, was STR profiled and tested negative for *Mycoplasma*. Cells were maintained in appropriate cell culture media (AsPC-1 and BxPC-3 – RPMI, CFPAC-1 – IMDM, HPAF-II – EMEM, MIA PaCa-2 – DMEM +2.5% Horse Serum, PANC-1 – DMEM) containing 10% fetal bovine serum (FBS) (R&D Systems; Minneapolis, MN) and 1% penicillin-streptomycin (Thermo Fisher; Waltham, MA) in a 37°C, 5% CO_2 incubator (HeraCell; Thermo Fisher). Experiments were performed on cells having undergone less than 20 passages. PDX lines (6164, 6741, 6413, 6182) were a generous gift from Dr. Debabrata (Dev) Mukhopadhyay (Mayo Clinic Jacksonville, FL). Lines were maintained in DMEM-F12 (Gibco) containing 20% FBS (R&D Systems, Minneapolis, MN) and 1% penicillin-streptomycin

(Thermo Fisher, Waltham, MA) in a 37°C, 5% CO_2 incubator (HeraCell, Thermo Fisher). PDX cells were not passaged more than six times prior to experimental use.

MTS assay

Analysis of viability 72 hpi with VSV or VMG was performed as previously described.[11] Briefly, cells were counted and viability assessed by trypan blue (Thermo Fisher, Waltham, MA) using the Luna-II Automated Cell Counter (Logos Biosystems, Annandale, VA). 1e4 viable cells were plated per well in 96-well plate format. Edge wells were not used for analysis to avoid edge effects. Cells were rested and allowed to adhere overnight before infection and/or treatment the next day. MTS (CellTiter96 Aqueous One) (Promega, Madison, WI) was added at 72 hpi and incubated for 1 h prior to reading the absorbance at 490 nm on a Synergy HTX plate reader (BioTek, Winooski, VT) using Gen5 version 3.12.08 software (Agilent Technologies).

Visualization of VMG-GFP infection

PDAC cells were plated in six-well plates at a density of 5e5 cells/well and rested overnight. The next day, cells were infected with MOI 1 of VMG-GFP. Cells were incubated with virus for 72 h. Phase and GFP fluorescence images were captured using an EVOS FL Auto microscope with ×10 lens magnification (×100 total). Total fluorescent area was quantified in ImageJ (NIH).

Viral replication kinetics

PDAC cells were plated at 5e5 cells per well in six-well plates. The next day they were infected with VSV, MorV, or VMG at an MOI 0.1 for 1 h before being washed with D-PBS (Thermo Fisher) and fresh cell culture media added. At 12, 24, 48, or 72 h after infection, 100 μL of supernatant was collected and stored at −80°C until assessment by plaque assay. For plaque assays, Vero cells were seeded in a 6-cm cell culture dish such that they were approximately 90% confluent at the time of infection. Cells were infected with 8-fold serial dilutions of supernatant in Opti-MEM for 1 h. Virus-containing media was aspirated, and cells were overlaid with 1.5% Agar + MEM +10% FBS. Following 72-h incubation at 37°C 5% CO_2, the agar was gently removed, and cells were stained with 1% crystal violet (Sigma) in 20% methanol to allow visualization of plaques. Plaques were counted manually at the dilution, which showed 10 to 100 plaques per plate and PFU/mL calculated by the dilution factor of that plate.

Syngeneic tumor model

Fourteen female C57BL/6 mice, 6–8 weeks old (Jackson Laboratories) were inoculated subcutaneously with 3e6 Pan02 cells in the right hind flank. After 7 days, mice were randomized into either the PBS or VMG-treated group. Mean tumor volume was 136 ± 6 mm^3 in both groups at this time (day 0). Intratumoral injection of 50 μL of PBS or 1e7 $TCID_{50}$ VMG in 50 μL was performed on day 0 and day 26. Body weight and tumor caliper measurements were taken every 2–3 days until study endpoint on day 32. Tumor volume was estimated using $V = 0.5 \times (Width^2 \times Length)$, where width was the shorter measurement across the tumor. Mice were euthanized if estimated tumor volume was >10% of body mass or if tumors ulcerated.

Animal husbandry

Animals were housed in HEPA ventilated cages (Innocage IVC, Innovive USA) with five mice per cage. Fluorescent lighting was provided on a 12-h cycle. Temperature and humidity were maintained to 68–74°F (20°C–23°C) and 30%–70% humidity. 2920X.10 18% soy irradiated rodent feed (Envigo) and autoclaved acidified water (pH2.5-3) were supplied *ad libitum*. Animal welfare was compliant with the U.S. Department of Agriculture's Animal Welfare Act (9 CFR Parts 1, 2 and 3). Protocol was Institutional Animal Care and Use Committee approved #CBSD-ACUP-001.

Serum liver enzyme quantification

Liver function tests were performed using 150 μL of undiluted mouse serum into a Dri-chem 4000 chemistry analyzer (Heska; Loveland, CO) using the Heska liver function panel cartridges according to the manufacturer's instructions.

Pan02 TIL analysis

TILs were isolated from resected tumors by tumor dissociation kit, mouse (Miltenyi, Cat#130-096-730) in gentleMACS C-tubes according to manufacturer's protocol. TILs were incubated with TruStain FcX (anti-mouse CD16/32) (BioLegend, Cat#101320) at 4°C for 15 min. Surface antibodies were added for 30 min at 4°C (Table S2) then washed with FACSWash. Fixation/Permeabilization (eBioscience, Cat#00–5521) was added for 30 min at RT in the dark then washed in 1x PermWash. Intracellular antibody (Ki67) was added for 30 min at RT. Cells were washed and resuspended in FACSWash. Data were immediately acquired on a BD LSRFortessa X-20 cytometer. Flow cytometry data were analyzed in FlowJo v.10.8.1 and v.10.9 (BD). Gating strategy is shown in Figure S3. Data were graphed in GraphPad Prism 9 for macOS (GraphPad Software). Statistical significance between treatment groups was performed by unpaired t test.

Pan02 IFNβ sensitivity

Assay was performed on Pan02 cells as previously described.[11] Cells were plated at 1e4 cells/well in a 96-well plate. The next day, cells were treated with dilutions of IFNβ (human: pbl assay science, Piscataway, NJ; mouse: R&D Systems, Minneapolis, MN) concurrently with VMG. Viability was assessed at 72 hpi by MTS.

DepMap RNA-seq analysis

Version 20Q4 CCLE RNA-seq read count data were downloaded from https://depmap.org/portal/. Expression data were normalized and filtered using the top 25% of the genes with the highest variance between sensitive and resistant groups. Differentially expressed genes (DEGs) were determined from read count data using non-parametric statistical analysis significance analysis of microarrays and RNA-seq (SAMseq). DEGs were run through GSEA and Enrichr databases for over-representation analysis. The biological categories and

corresponding gene sets were extracted from MSigDB (V7.2): KEGG, REACTOME, BIOCARTA, PID, HALLMARK GENES, and Gene Ontology (GO) Biological Processes.

Proteomic analysis

CFPAC-1 and MIA PaCa-2 were plated in 8 × 150-mm Corning cell culture plates per cell line in complete medium. When cells were 80%–90% confluent, they were infected with VMG at MOI 0.1 or mock as a control, four plates per condition. At 18 hpi, plates were washed with PBS and cells were scraped into a 2-mL microcentrifuge tube per plate on ice. Cells were lysed in 1x RIPA buffer containing PMSF and vortexed periodically while incubating on ice for 20 min. Tubes were centrifuged 12,000 rpm × 15 min at 4°C. Supernatant was collected into a new labeled tube. Protein was quantified by BCA assay and samples were stored at −80°C until shipment. Protein samples were shipped overnight on dry ice to IDeA National Resource for Quantitative Proteomics at UAMS. Protein was extracted by chloroform/methanol extraction and trypsin digested, and TMT labeling performed. High pH peptide fractionation (18 super-fractions) was performed by bHPLC. Data acquisition was by an Orbitrap Eclipse mass spectrometer (TMT MS3; 60 min gradient per fraction). Proteins were identified by MaxQuant. Statistical analysis was performed by limma.

Derivation of resistant cells

PDAC cells were plated at 5e5 cells per well in 3-mL appropriate cell culture media in tissue-culture-treated six-well plates. Cells were rested for 48 h prior to starting the assay. On the day of the assay, live cells were estimated to be 1e6 cells per well and were infected at MOI 0.1 of VSV in Opti-MEM media. One hour post-infection, media was aspirated from wells and cells were washed with PBS. Fresh Opti-MEM media was added to all wells and cells were maintained in a humidified cell culture incubator for 72 h. On day 3 post-infection, cells were collected for RNA and protein (Infection 1: I1). Other replicate wells were re-infected using the same protocol (infected, washed 1 hpi, cultured for 3 days) before RNA and protein sample collection (I2).

Derived resistance RNA-seq

Derived resistant or control cells were collected in 200 μL of RNAProtect reagent (Qiagen) was added to each well and incubated for 3 min at RT. Cells were collected into labeled microtubes and stored at −80°C until extraction. RNA was extracted using QIAshredder (Qiagen) followed by RNeasy Mini Kit (Qiagen) according to the manufacturer's recommendations. RNA quantity and quality were assessed before shipping samples on dry ice overnight to Novogene for DNase treatment and sequencing. CFPAC-1 Ctrl, CFPAC-1 I2, and BxPC-3 Ctrl were assessed in duplicate. BxPC-3 I1, BxPC-3 I2, CFPAC-1 I1, Capan-2 Ctrl, and Capan-2 I2 were assessed in individual samples. CFPAC-1 data were analyzed using ExpressAnalyst (https://www.expressanalyst.ca/). Low abundance and variance percentile lower than 15% features were filtered. Data were normalized by Log2-counts per million and DEGs were determined by DESeq2. For heatmap expression comparisons, read counts from BxPC-3, Capan-2, and CFPAC-1 samples were normalized to counts per million (CPM). Heatmaps were generated in Prism v.9 (GraphPad).

DATA AND CODE AVAILABILITY

The data that support the findings of this study are available from the corresponding author (borad.mitesh@mayo.edu) upon reasonable request. Data are stored with controlled access on Mayo Clinic secure servers.

ACKNOWLEDGMENTS

The authors thank CrownBio for assistance with *in vivo* work. We thank the IDeA National Resource for Quantitative Proteomics at UAMS for their assistance in planning and executing proteomics evaluations. Several PDAC lines were a generous gift from Dr. Martin Fernandez-Zapico. PDX cell lines were kindly provided by Dr. Debabrata (Dev) Mukhopadhyay. This project was partially funded through a Research Completion Award made possible through the Geographical Management of Cancer Health Disparities Program (GMaP) Region 3, an initiative of the National Cancer Institute's Center to Reduce Cancer Health Disparities (to C.R.W.), and a Mayo Clinic Department of Molecular Medicine Small Grant (to C.R.W.). This work was supported by National Institutes of Health (NIH) through a K01 award CA234324 (to B.M.N.), American Association for Cancer Research (AACR) grant (to B.M.N.), Start-up from the Winthrop P. Rockefeller Cancer Institute (to B.M.N.), National Cancer Institute (NCI) K12 award CA090628 (to M.J.B.), the Mayo Clinic Hepatobiliary SPORE P50CA210964 (to M.J.B.), Mayo Clinic Cancer Center CCSG Gene and Virus Therapy program grant (to M.J.B.), and NIH DP2CA301099 (to B.M.N). The IDeA National Resource for Quantitative Proteomics is supported by NIGMS grant R24GM137786. The funders had no role in study design, data collection and interpretation, or the decision to submit the work for publication.

AUTHOR CONTRIBUTIONS

Conceptualization, C.R.W., M.J.B., and B.M.N.; Methodology, C.R.W., O.B., M.G., M.Y.M., N.M.E., E.A.R., B.M.N., and M.J.B.; Investigation, C.R.W., O.B., and M.Y.M.; Visualization, C.R.W., O.B., M.G., and M.Y.M.; Writing – Original Draft, C.R.W.; Writing – Review & Editing, C.R.W., O.B., M.G., M.Y.M., N.M.E., E.A.R., K.H.B., M.Z.T., O.M., K.U.F.., Y.Z., M.T.B., B.M.N., and M.J.B.; Funding Acquisition, C.R.W., B.M.N., and M.J.B.; Resources, B.M.N. and M.J.B; Supervision, B.M.N. and M.J.B.

DECLARATION OF INTERESTS

The authors declare no competing interests.

SUPPLEMENTAL INFORMATION

Supplemental information can be found online at https://doi.org/10.1016/j.omton.2025.200937.

REFERENCES

1. Haller, S.D., Monaco, M.L., and Essani, K. (2020). The Present Status of Immuno-Oncolytic Viruses in the Treatment of Pancreatic Cancer. Viruses *12*, 1318. https://doi.org/10.3390/v12111318.

2. Von Hoff, D.D., Ervin, T., Arena, F.P., Chiorean, E.G., Infante, J., Moore, M., Seay, T., Tjulandin, S.A., Ma, W.W., Saleh, M.N., et al. (2013). Increased survival in pancreatic cancer with nab-paclitaxel plus gemcitabine. N. Engl. J. Med. *369*, 1691–1703. https://doi.org/10.1056/NEJMoa1304369.

3. Nisar, M., Paracha, R.Z., Adil, S., Qureshi, S.N., and Janjua, H.A. (2022). An Extensive Review on Preclinical and Clinical Trials of Oncolytic Viruses Therapy for Pancreatic Cancer. Front. Oncol. *12*, 875188. https://doi.org/10.3389/fonc.2022.875188.

4. Torphy, R.J., Schulick, R.D., and Zhu, Y. (2020). Understanding the immune landscape and tumor microenvironment of pancreatic cancer to improve immunotherapy. Mol. Carcinog. *59*, 775–782. https://doi.org/10.1002/mc.23179.

5. Muller, M., Haghnejad, V., Schaefer, M., Gauchotte, G., Caron, B., Peyrin-Biroulet, L., Bronowicki, J.-P., Neuzillet, C., and Lopez, A. (2022). The Immune Landscape of Human Pancreatic Ductal Carcinoma: Key Players, Clinical Implications, and Challenges. Cancers *14*, 995. https://doi.org/10.3390/cancers14040995.

6. Bulle, A., and Lim, K.-H. (2020). Beyond just a tight fortress: contribution of stroma to epithelial-mesenchymal transition in pancreatic cancer. Signal Transduct. Targeted Ther. *5*, 249. https://doi.org/10.1038/s41392-020-00341-1.

7. Hilmi, M., Bartholin, L., and Neuzillet, C. (2018). Immune therapies in pancreatic ductal adenocarcinoma: Where are we now? World J. Gastroenterol. *24*, 2137–2151. https://doi.org/10.3748/wjg.v24.i20.2137.

8. Hamidi-Sofiani, V., Rakhshi, R., Moradi, N., Zeynali, P., Nakhaie, M., and Behboudi, E. (2022). Oncolytic viruses and pancreatic cancer. Cancer Treat. Res. Commun. *31*, 100563. https://doi.org/10.1016/j.ctarc.2022.100563.

9. Hastie, E., and Grdzelishvili, V.Z. (2012). Vesicular stomatitis virus as a flexible platform for oncolytic virotherapy against cancer. J. Gen. Virol. *93*, 2529–2545. https://doi.org/10.1099/vir.0.046672-0.

10. Holbrook, M.C., Goad, D.W., and Grdzelishvili, V.Z. (2021). Expanding the Spectrum of Pancreatic Cancers Responsive to Vesicular Stomatitis Virus-Based Oncolytic Virotherapy: Challenges and Solutions. Cancers *13*, 1171. https://doi.org/10.3390/cancers13051171.

11. Rihn, S.J., Aziz, M.A., Stewart, D.G., Hughes, J., Turnbull, M.L., Varela, M., Sugrue, E., Herd, C.S., Stanifer, M., Sinkins, S.P., et al. (2019). TRIM69 Inhibits Vesicular Stomatitis Indiana Virus. J. Virol. *93*, e00951-19. https://doi.org/10.1128/JVI.00951-19.

12. Kueck, T., Bloyet, L.-M., Cassella, E., Zang, T., Schmidt, F., Brusic, V., Tekes, G., Pornillos, O., Whelan, S.P.J., and Bieniasz, P.D. (2019). Vesicular Stomatitis Virus Transcription Is Inhibited by TRIM69 in the Interferon-Induced Antiviral State. J. Virol. *93*, e01372-19. https://doi.org/10.1128/JVI.01372-19.

13. Matveeva, O.V., and Chumakov, P.M. (2018). Defects in interferon pathways as potential biomarkers of sensitivity to oncolytic viruses. Rev. Med. Virol. *28*, e2008. https://doi.org/10.1002/rmv.2008.

14. Westcott, M.M., Liu, J., Rajani, K., D'Agostino Jr, R., Lyles, D.S., and Porosnicu, M. (2015). Interferon Beta and Interferon Alpha 2a Differentially Protect Head and Neck Cancer Cells from Vesicular Stomatitis Virus-Induced Oncolysis. J. Virol. *89*, 7944–7954. https://doi.org/10.1128/JVI.00757-15.

15. Blackham, A.U., Northrup, S.A., Willingham, M., Sirintrapun, J., Russell, G.B., Lyles, D.S., and Stewart, J.H., 4th (2014). Molecular determinants of susceptibility to oncolytic vesicular stomatitis virus in pancreatic adenocarcinoma. J. Surg. Res. *187*, 412–426. https://doi.org/10.1016/j.jss.2013.10.032.

16. Janelle, V., Brassard, F., Lapierre, P., Lamarre, A., and Poliquin, L. (2011). Mutations in the glycoprotein of vesicular stomatitis virus affect cytopathogenicity: potential for oncolytic virotherapy. J. Virol. *85*, 6513–6520. https://doi.org/10.1128/JVI.02484-10.

17. Jenks, N., Myers, R., Greiner, S.M., Thompson, J., Mader, E.K., Greenslade, A., Griesmann, G.E., Federspiel, M.J., Rakela, J., Borad, M.J., et al. (2010). Safety studies on intrahepatic or intratumoral injection of oncolytic vesicular stomatitis virus expressing interferon-beta in rodents and nonhuman primates. Hum. Gene Ther. *21*, 451–462. https://doi.org/10.1089/hum.2009.111.

18. Faul, E.J., Wanjalla, C.N., McGettigan, J.P., and Schnell, M.J. (2008). Interferon-beta expressed by a rabies virus-based HIV-1 vaccine vector serves as a molecular adjuvant and decreases pathogenicity. Virology *382*, 226–238. https://doi.org/10.1016/j.virol.2008.09.019.

19. Wollmann, G., Robek, M.D., and van den Pol, A.N. (2007). Variable deficiencies in the interferon response enhance susceptibility to vesicular stomatitis virus oncolytic actions in glioblastoma cells but not in normal human glial cells. J. Virol. *81*, 1479–1491. https://doi.org/10.1128/JVI.01861-06.

20. Basu, M., Maitra, R.K., Xiang, Y., Meng, X., Banerjee, A.K., and Bose, S. (2006). Inhibition of vesicular stomatitis virus infection in epithelial cells by alpha interferon-induced soluble secreted proteins. J. Gen. Virol. *87*, 2653–2662. https://doi.org/10.1099/vir.0.82039-0.

21. Obuchi, M., Fernandez, M., and Barber, G.N. (2003). Development of recombinant vesicular stomatitis viruses that exploit defects in host defense to augment specific oncolytic activity. J. Virol. *77*, 8843–8856. https://doi.org/10.1128/jvi.77.16.8843-8856.2003.

22. Watters, C.R., Barro, O., Elliott, N.M., Zhou, Y., Gabere, M., Raupach, E., Baker, A.T., Barrett, M.T., Buetow, K.H., Jacobs, B., et al. (2023). Multi-modal efficacy of a chimeric vesiculovirus expressing the Morreton glycoprotein in sarcoma. Mol. Ther. Oncolytics *29*, 4–14. https://doi.org/10.1016/j.omto.2023.02.009.

23. Carroll, A.R., and Wagner, R.R. (1979). Role of the membrane (M) protein in endogenous inhibition of *in vitro* transcription by vesicular stomatitis virus. J. Virol. *29*, 134–142. https://doi.org/10.1128/JVI.29.1.134-142.1979.

24. Nagalo, B.M., Zhou, Y., Loeuillard, E.J., Dumbauld, C., Barro, O., Elliott, N.M., Baker, A.T., Arora, M., Bogenberger, J.M., Meurice, N., et al. (2023). Characterization of Morreton virus as an oncolytic virotherapy platform for liver cancers. Hepatology *77*, 1943–1957. https://doi.org/10.1002/hep.32769.

25. Liu, Y.-P., Suksanpaisan, L., Steele, M.B., Russell, S.J., and Peng, K.-W. (2013). Induction of antiviral genes by the tumor microenvironment confers resistance to virotherapy. Sci. Rep. *3*, 2375. https://doi.org/10.1038/srep02375.

26. Uhlen, M., Zhang, C., Lee, S., Sjöstedt, E., Fagerberg, L., Bidkhori, G., Benfeitas, R., Arif, M., Liu, Z., Edfors, F., et al. (2017). A pathology atlas of the human cancer transcriptome. Science *357*, eaan2507. https://doi.org/10.1126/science.aan2507.

27. Cermelli, C., Cuoghi, A., Scuri, M., Bettua, C., Neglia, R.G., Ardizzoni, A., Blasi, E., Iannitti, T., and Palmieri, B. (2011). In vitro evaluation of antiviral and virucidal activity of a high molecular weight hyaluronic acid. Virol. J. *8*, 141. https://doi.org/10.1186/1743-422X-8-141.

28. Dickreuter, E., and Cordes, N. (2017). The cancer cell adhesion resistome: mechanisms, targeting and translational approaches. Biol. Chem. *398*, 721–735. https://doi.org/10.1515/hsz-2016-0326.

29. Shaw, A.E., Hughes, J., Gu, Q., Behdenna, A., Singer, J.B., Dennis, T., Orton, R.J., Varela, M., Gifford, R.J., Wilson, S.J., and Palmarini, M. (2017). Fundamental properties of the mammalian innate immune system revealed by multispecies comparison of type I interferon responses. PLoS Biol. *15*, e2004086. https://doi.org/10.1371/journal.pbio.2004086.

30. Noyce, R.S., and Richardson, C.D. (2012). Nectin 4 is the epithelial cell receptor for measles virus. Trends Microbiol. *20*, 429–439. https://doi.org/10.1016/j.tim.2012.05.006.

31. Jerabek, I., Zechmeister-Machhart, M., Binder, B.R., and Geiger, M. (2001). Binding of retinoic acid by the inhibitory serpin protein C inhibitor. Eur. J. Biochem. *268*, 5989–5996. https://doi.org/10.1046/j.0014-2956.2001.02560.x.

32. Zhan, Y., Jiang, L., Jin, X., Ying, S., Wu, Z., Wang, L., Yu, W., Tong, J., Zhang, L., Lou, Y., and Qiu, Y. (2021). Inhibiting RRM2 to enhance the anticancer activity of chemotherapy. Biomed. Pharmacother. *133*, 110996. https://doi.org/10.1016/j.biopha.2020.110996.

33. De Las Rivas, J., Brozovic, A., Izraely, S., Casas-Pais, A., Witz, I.P., and Figueroa, A. (2021). Cancer drug resistance induced by EMT: novel therapeutic strategies. Arch. Toxicol. *95*, 2279–2297. https://doi.org/10.1007/s00204-021-03063-7.

34. Szklarczyk, D., Kirsch, R., Koutrouli, M., Nastou, K., Mehryary, F., Hachilif, R., Gable, A.L., Fang, T., Doncheva, N.T., Pyysalo, S., et al. (2023). The STRING database in 2023: protein-protein association networks and functional enrichment analyses for any sequenced genome of interest. Nucleic Acids Res. *51*, D638–D646. https://doi.org/10.1093/nar/gkac1000.

35. Bhatt, D.K., Chammas, R., and Daemen, T. (2021). Resistance Mechanisms Influencing Oncolytic Virotherapy, a Systematic Analysis. Vaccines *9*, 1166. https://doi.org/10.3390/vaccines9101166.

36. Patel, M.R., Dash, A., Jacobson, B.A., Ji, Y., Baumann, D., Ismail, K., and Kratzke, R.A. (2019). JAK/STAT inhibition with ruxolitinib enhances oncolytic virotherapy in non-small cell lung cancer models. Cancer Gene Ther. *26*, 411–418. https://doi.org/10.1038/s41417-018-0074-6.

37. Morosi, L., Meroni, M., Ubezio, P., Fuso Nerini, I., Minoli, L., Porcu, L., Panini, N., Colombo, M., Blouw, B., Kang, D.W., et al. (2021). PEGylated recombinant human hyaluronidase (PEGPH20) pre-treatment improves intra-tumour distribution and efficacy of paclitaxel in preclinical models. J. Exp. Clin. Cancer Res. *40*, 286. https://doi.org/10.1186/s13046-021-02070-x.

38. Infante, J.R., Korn, R.L., Rosen, L.S., LoRusso, P., Dychter, S.S., Zhu, J., Maneval, D.C., Jiang, P., Shepard, H.M., Frost, G., et al. (2018). Phase 1 trials of PEGylated recombinant human hyaluronidase PH20 in patients with advanced solid tumours. Br. J. Cancer *118*, 153–161. https://doi.org/10.1038/bjc.2017.327.

39. Kultti, A., Zhao, C., Singha, N.C., Zimmerman, S., Osgood, R.J., Symons, R., Jiang, P., Li, X., Thompson, C.B., Infante, J.R., et al. (2014). Accumulation of extracellular hyaluronan by hyaluronan synthase 3 promotes tumor growth and modulates the

pancreatic cancer microenvironment. BioMed Res. Int. *2014*, 817613. https://doi.org/10.1155/2014/817613.

40. Moerdyk-Schauwecker, M., Shah, N.R., Murphy, A.M., Hastie, E., Mukherjee, P., and Grdzelishvili, V.Z. (2013). Resistance of pancreatic cancer cells to oncolytic vesicular stomatitis virus: role of type I interferon signaling. Virology *436*, 221–234. https://doi.org/10.1016/j.virol.2012.11.014.

41. Ahn, E., Araki, K., Hashimoto, M., Li, W., Riley, J.L., Cheung, J., Sharpe, A.H., Freeman, G.J., Irving, B.A., and Ahmed, R. (2018). Role of PD-1 during effector CD8 T cell differentiation. Proc. Natl. Acad. Sci. USA *115*, 4749–4754. https://doi.org/10.1073/pnas.1718217115.

42. MEAGER, A., VISVALINGAM, K., DILGER, P., BRYAN, D., and WADHWA, M. (2005). Biological activity of interleukins-28 and -29: Comparison with type I interferons. Cytokine *31*, 109–118. https://doi.org/10.1016/j.cyto.2005.04.003.

43. Sommereyns, C., Paul, S., Staeheli, P., and Michiels, T. (2008). IFN-lambda (IFN-lambda) is expressed in a tissue-dependent fashion and primarily acts on epithelial cells *in vivo*. PLoS Pathog. *4*, e1000017. https://doi.org/10.1371/journal.ppat.1000017.

44. Lazear, H.M., Schoggins, J.W., and Diamond, M.S. (2019). Shared and Distinct Functions of Type I and Type III Interferons. Immunity *50*, 907–923. https://doi.org/10.1016/j.immuni.2019.03.025.

45. Guayasamin, R.C., Reynolds, T.D., Wei, X., Fujiwara, M., and Robek, M.D. (2014). Type III interferon attenuates a vesicular stomatitis virus-based vaccine vector. J. Virol. *88*, 10909–10917. https://doi.org/10.1128/JVI.01910-14.

46. Wongthida, P., Diaz, R.M., Galivo, F., Kottke, T., Thompson, J., Pulido, J., Pavelko, K., Pease, L., Melcher, A., and Vile, R. (2010). Type III IFN interleukin-28 mediates the antitumor efficacy of oncolytic virus VSV in immune-competent mouse models of cancer. Cancer Res. *70*, 4539–4549. https://doi.org/10.1158/0008-5472.CAN-09-4658.

47. Hattori, N., Komine, M., Yano, S., Kaneko, T., Hanakawa, Y., Hashimoto, K., and Tamaki, K. (2002). Interferon-γ, a Strong Suppressor of Cell Proliferation, Induces Upregulation of Keratin K6, One of the Inflammatory- and Proliferation-Associated Keratins. J. Invest. Dermatol. *119*, 403–410. https://doi.org/10.1046/j.1523-1747.2002.01843.x.

48. Hastie, E., Besmer, D.M., Shah, N.R., Murphy, A.M., Moerdyk-Schauwecker, M., Molestina, C., Roy, L.D., Curry, J.M., Mukherjee, P., and Grdzelishvili, V.Z. (2013). Oncolytic vesicular stomatitis virus in an immunocompetent model of MUC1-positive or MUC1-null pancreatic ductal adenocarcinoma. J. Virol. *87*, 10283–10294. https://doi.org/10.1128/JVI.01412-13.

49. Dhar, P., and McAuley, J. (2019). The Role of the Cell Surface Mucin MUC1 as a Barrier to Infection and Regulator of Inflammation. Front. Cell. Infect. Microbiol. *9*, 117. https://doi.org/10.3389/fcimb.2019.00117.

50. McAuley, J.L., Corcilius, L., Tan, H.-X., Payne, R.J., McGuckin, M.A., and Brown, L.E. (2017). The cell surface mucin MUC1 limits the severity of influenza A virus infection. Mucosal Immunol. *10*, 1581–1593. https://doi.org/10.1038/mi.2017.16.

51. Walters, R.W., Pilewski, J.M., Chiorini, J.A., and Zabner, J. (2002). Secreted and Transmembrane Mucins Inhibit Gene Transfer with AAV4 More Efficiently than AAV5. J. Biol. Chem. *277*, 23709–23713. https://doi.org/10.1074/jbc.m200292200.

52. Winter, J.M., Tang, L.H., Klimstra, D.S., Brennan, M.F., Brody, J.R., Rocha, F.G., Jia, X., Qin, L.-X., D'Angelica, M.I., DeMatteo, R.P., et al. (2012). A novel survival-based tissue microarray of pancreatic cancer validates MUC1 and mesothelin as biomarkers. PLoS One *7*, e40157. https://doi.org/10.1371/journal.pone.0040157.

53. Mayado, A., Orfao, A., Mentink, A., Gutierrez, M.L., Muñoz-Bellvis, L., and Terstappen, L.W.M.M. (2020). Detection of circulating tumor cells in blood of pancreatic ductal adenocarcinoma patients. Cancer Drug Resist. *3*, 83–97. https://doi.org/10.20517/cdr.2019.73.

54. Boivin, M., Lane, D., Piché, A., and Rancourt, C. (2009). CA125 (MUC16) tumor antigen selectively modulates the sensitivity of ovarian cancer cells to genotoxic drug-induced apoptosis. Gynecol. Oncol. *115*, 407–413. https://doi.org/10.1016/j.ygyno.2009.08.007.

55. Bierie, B., Pierce, S.E., Kroeger, C., Stover, D.G., Pattabiraman, D.R., Thiru, P., Liu Donaher, J., Reinhardt, F., Chaffer, C.L., Keckesova, Z., and Weinberg, R.A. (2017). Integrin-β4 identifies cancer stem cell-enriched populations of partially mesenchymal carcinoma cells. Proc. Natl. Acad. Sci. USA *114*, E2337–E2346. https://doi.org/10.1073/pnas.1618298114.

56. (2023). Human Protein Atlas. https://www.proteinatlas.org/.

57. Hastie, E., Cataldi, M., Moerdyk-Schauwecker, M.J., Felt, S.A., Steuerwald, N., and Grdzelishvili, V.Z. (2016). Novel biomarkers of resistance of pancreatic cancer cells to oncolytic vesicular stomatitis virus. Oncotarget *7*, 61601–61618. https://doi.org/10.18632/oncotarget.11202.

58. Tang, Q., Wu, L., Xu, M., Yan, D., Shao, J., and Yan, S. (2020). Osalmid, a Novel Identified RRM2 Inhibitor, Enhances Radiosensitivity of Esophageal Cancer. Int. J. Radiat. Oncol. Biol. Phys. *108*, 1368–1379. https://doi.org/10.1016/j.ijrobp.2020.07.2322.

59. Liu, X., Deng, J., Yuan, Y., Chen, W., Sun, W., Wang, Y., Huang, H., Liang, B., Ming, T., Wen, J., et al. (2022). Advances in Trop2-targeted therapy: Novel agents and opportunities beyond breast cancer. Pharmacol. Ther. *239*, 108296. https://doi.org/10.1016/j.pharmthera.2022.108296.

60. Song, T.-J., Haddad, D., Adusumilli, P., Kim, T., Stiles, B., Hezel, M., Socci, N.D., Gönen, M., and Fong, Y. (2012). Molecular network pathways and functional analysis of tumor signatures associated with development of resistance to viral gene therapy. Cancer Gene Ther. *19*, 38–48. https://doi.org/10.1038/cgt.2011.64.

61. Kinker, G.S., Greenwald, A.C., Tal, R., Orlova, Z., Cuoco, M.S., McFarland, J.M., Warren, A., Rodman, C., Roth, J.A., Bender, S.A., et al. (2020). Pan-cancer single-cell RNA-seq identifies recurring programs of cellular heterogeneity. Nat. Genet. *52*, 1208–1218. https://doi.org/10.1038/s41588-020-00726-6.